Fig. 6.   Schematic of mixed-mode simulation of asymmetric coupled-pair transmission line.
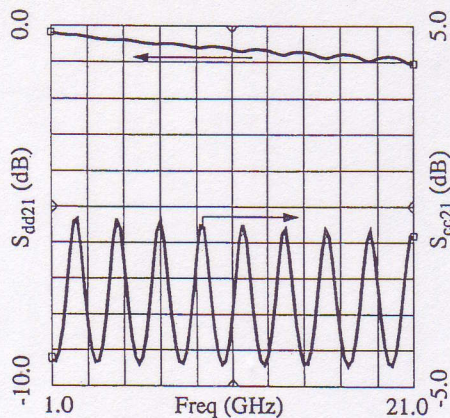

Fig. 8.   Simulated magnitude in dB of S_{dd11} and S_{cc11} versus frequency for asymmetric coupled-pair line.

Fig. 7.   Simulated magnitude in dB of S_{dd21} and S_{cc21} versus frequency for asymmetric coupled-pair line.

shows significant conversion between propagation modes, particularly in transmission parameters S_{dc21} and S_{cd21}. Note these two sub-matrices are equal indicating equal conversion from differential to common-mode and from common to differential-mode. These non-zero s-parameters can be interpreted conceptually in the following way. In the case of S_{cd21}, a pure differential mode wave is impinging on port 1 of the DUT. However, at port 2, both differential and common-mode waves exist. Some of the energy of the differential wave is converted to a common-mode propagation, and the total energy is preserved (except for losses in the metal and dielectric).

This example circuit was simulated across frequency, and the magnitudes of selected mixed-mode s-parameters are plotted in Figs. 7–10. Fig. 7 shows both S_{dd21} and S_{cc21} in dB from 1–21 GHz. The ripple pattern across frequency in the common-mode transmission (S_{cc21}) indicates an impedance mismatch at the ports for common-mode propagation. At the higher frequencies of the plot, the finite conductivity of the conductors is evident as average loss increases. The differential-mode transmission (S_{dd21}) shows smaller ripples (0.2-dB maximum), indicating smaller mismatch, and also shows lower average loss. However, the losses due to the reflections at the ports do not account for all of the ripple in the differential transmission. As can be seen in Fig. 8, the return loss for the differential mode is greater than 20 dB, which can account for approximately 0.04 dB of worst case loss (over ohmic losses). Mode conversion accounts for the remaining reduction in the differential-mode, and hence S_{dd21} is reduced. Here, differential energy is converted to both common-mode transmission S_{cd21} and common-mode reflection S_{cd11}. Fig. 9 shows the cross-mode transmission S_{cd21} in dB, and Fig. 10 shows the cross-mode reflection S_{cd11} in dB. The minima in

circuitry, is shown in Fig. 6. One top conductor width is 100 μm, and the second is 170 μm, with an edge-to-edge spacing of 65 μm. Again, the substrate is 25-mil-thick alumina with a relative permittivity of 9.6 with a loss tangent of 0.001, and the metal conductivity is that of copper. A one inch section of this line was simulated in MDS at 5 GHz, and the mixed-mode s-parameters are shown in (28) at the bottom of the page.

As in the first example, each partitioned sub-matrix demonstrates the properties of a reciprocal, passive and (port) symmetric DUT. Also like the first example, the differential s-parameters show the coupled pair possesses an odd-mode characteristic impedance of nearly 50 Ω (actually 49 Ω), and has low-loss propagation in the differential mode. The common-mode s-parameters show the coupled pair has a greater degree of mismatch than the first example (the even-mode impedance is 152 Ω in this case).

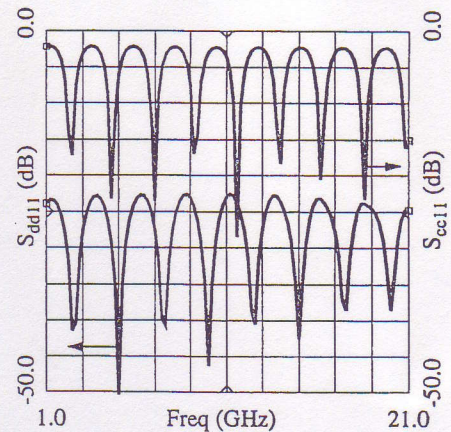The most important difference between the two examples is seen in the cross-mode s-parameters. The data in (28)

$$\left[\begin{array}{c|c} S_{dd} & S_{dc} \\ \hline S_{cd} & S_{cc} \end{array}\right] = \left[\begin{array}{cc|cc} 0.003\angle{-175}° & 0.956\angle{1.819}° & 0.005\angle{-177}° & 0.031\angle{80.7}° \\ 0.956\angle{1.819}° & 0.003\angle{-175}° & 0.031\angle{80.7}° & 0.005\angle{-177}° \\ \hline 0.005\angle{-177}° & 0.031\angle{80.7}° & 0.502\angle{48.0}° & 0.844\angle{-40.2}° \\ 0.031\angle{80.7}° & 0.005\angle{-177}° & 0.844\angle{-40.2}° & 0.502\angle{-48.0}° \end{array}\right]. \tag{28}$$